Correlation methods in optical metrology with state-of-the-art x-ray mirrors

Valeriy V. Yashchuk*, Gary Centers, Gevork S. Gevorkyan, Ian Lacey, and Brian V. Smith
Lawrence Berkeley National Laboratory, One Cyclotron Rd., Berkeley, California 94720, USA

ABSTRACT

The development of fully coherent free electron lasers and diffraction limited storage ring x-ray sources has brought to focus the need for higher performing x-ray optics with unprecedented tolerances for surface slope and height errors and roughness. For example, the proposed beamlines for the future upgraded Advance Light Source, ALS-U, require optical elements characterized by a residual slope error of <100 nrad (root-mean-square) and height error of <1-2 nm (peak-to-valley). These are for optics with a length of up to one meter. However, the current performance of x-ray optical fabrication and metrology generally falls short of these requirements. The major limitation comes from the lack of reliable and efficient surface metrology with required accuracy and with reasonably high measurement rate, suitable for integration into the modern deterministic surface figuring processes. The major problems of current surface metrology relate to the inherent instrumental temporal drifts, systematic errors, and/or an unacceptably high cost, as in the case of interferometry with computer-generated holograms as a reference. In this paper, we discuss the experimental methods and approaches based on correlation analysis to the acquisition and processing of metrology data developed at the ALS X-Ray Optical Laboratory (XROL). Using an example of surface topography measurements of a state-of-the-art x-ray mirror performed at the XROL, we demonstrate the efficiency of combining the developed experimental correlation methods to the advanced optimal scanning strategy (AOSS) technique. This allows a significant improvement in the accuracy and capacity of the measurements via suppression of the instrumental low frequency noise, temporal drift, and systematic error in a single measurement run. Practically speaking, implementation of the AOSS technique leads to an increase of the measurement accuracy, as well as the capacity of ex situ metrology by a factor of about four. The developed method is general and applicable to a broad spectrum of high accuracy measurements.

Keywords: correlation analysis, optical scanning strategy, optimization algorithms, measurement errors, systematic errors, drift error, random noise, x-ray optics, surface metrology

1. INTRODUCTION

The development of fully coherent free electron lasers, and diffraction limited storage ring x-ray sources has brought to a focus the need for higher performing x-ray optics with unprecedented tolerances for surface slope and height errors and roughness. For example, the proposed beamlines for the future upgraded Advance Light Source, ALS-U,[1,2] require optical elements characterized by a residual slope error of <100 nrad rms (root-mean-square) and height error of <1-2 nm P-V (peak-to-valley) for optics with a length of up to one meter.[3-7]

The current performance of x-ray optical fabrication and metrology generally falls short of these requirements (see, for example, Ref.[8] and references therein). The major limitation comes from the lack of reliable and efficient surface metrology with required accuracy and with reasonably high measurement rate, suitable for integration into the modern deterministic surface figuring processes. The current metrology tools in use at the x-ray facilities, as well as in the optical industry, include those that perform traditional long trace profilometry,[9-18] auto-collimator (AC) based surface deflectometry,[19-27] and interferometry,[27-30] and have basically reached their limits. These limits are mostly determined by the inherent instrumental temporal drifts, systematic errors, and/or an unacceptably high cost, as in the case of interferometry with computer-generated holograms as a reference.[31-36] Due to the extreme tolerances required, the very specific nature of metrology for x-ray optics, and the relatively small market, it increasingly falls on metrology team at x-ray facilities to develop the required metrology, while carrying out their normal role of qualifying optical systems for use in beamlines (see, for example, Refs.[37-39] and references therein).

*vvyaschuk@lbl.gov; phone 1 510 495-2592; fax 1 510 486-7696

There are three general directions for improvement of accuracy of measurements in experimental physics and industry, including ex situ (in the lab) metrology for state-of-the-art x-ray optics. The most radical and expensive direction is the development of new high performance measurement instruments and calibration tools. This requires a deep revision of the basic schematics and principles placed in the foundation of these instruments and tools, and, therefore, significant time, monetary, and manpower resources for the research and development.

In spite of the remarkable achievements (for review see, for example, Refs.[8,40-48] and references therein), the current accuracy of metrology instruments, available at the x-ray facilities, is often limited by drift errors of the measurements due to temporal instabilities of the experimental arrangement and systematic errors inherent to the instruments. Both are very tightly dependent on the laboratory's environmental conditions. Therefore, the second direction for metrology improvement is building of advanced environmental control that is a key component in the development of ultra-high accuracy ex situ metrology.[49,50]

The direction most efficient from the point of view of the required funding and achievable advantages is the development and implementation of innovative experimental measurement methods for optimal usage (with the highest possible accuracy) of the capabilities (inherent precision and stability) of the existing instrumentation within the available environmental conditions.[51-57]

In this paper, we present and discuss the experimental methods and approaches, based on correlation analysis, to the acquisition and processing of metrology data developed and used at the ALS X-Ray Optical Laboratory (XROL).[49,50] Using an example of surface topography measurements with a state-of-the-art x-ray mirror performed at the XROL, we demonstrate the efficiency of the developed experimental methods to significantly improve the accuracy of the measurement via suppression of the instrumental low frequency noise, temporal drift, and systematic error. The developed methods are general and applicable to a broad spectrum of high accuracy measurements in experimental science and industry.

This paper is organized as follows: First, in Sec. 2 we briefly analyze the error sources affecting the accuracy of optical tools for metrology with x-ray optics. The drift error suppression method based on optimal scanning strategies (OSS), first suggested in Ref.[53] and recently extended to 2D slope profiling,[57] is briefly reviewed in Sec. 3. An original procedure developed to suppress the measurement errors associated with periodic temporal variation of the environmental conditions is presented in Sec. 4. Section 5 provides mathematical foundations of the correlation methods, introduced in surface metrology practice in Refs.,[51-53,55] for suppression of systematic errors. In Sec. 6, we firstly present the advanced OSS (AOSS) technique that allows incorporating in one measurement run the advantages of the methods for suppression of the drift and systematic errors used originally with a number of sequential runs. A realization of the developed advanced method in the high accuracy surface slope measurements with a hyperbolic x-ray mirror is described in Sec. 7. In this case, the implementation of the AOSS techniques leads to an increase of the measurement accuracy, as well as the throughput capacity of ex situ metrology by a factor of about four. The paper concludes (Sec. 8) by summarizing the main concepts discussed throughout the paper and by stating a plan for the incorporation of the developed method in the slope measurement profilers under development at the ALS XROL. Despite the fact that this paper is focused on measurements with surface slope profilers available at the ALS XROL: long trace profilers, upgraded LTP-II,[15] the Developmental LTP,[22] and a new Optical Surface Measuring System, OSMS[57] (the last two are the AC based deflectometers), the analysis and the developed method are applicable to a broad spectrum of high accuracy optical and physical measurements in general.

2. THE ERRORS OF MEASUREMENTS WITH SURFACE SLOPE PROFILERS

Figure 1 depicts a schematic of the experimental arrangement for surface slope profiling based on an AC as an angular (surface slope) sensor and a movable pentaprism for scanning the sample beam along the surface under test (SUT). The coordinate system's origin is placed at the center of the mirror's clear aperture (CA).

A surface slope profile measured in a single measurement, $\alpha_i^M \equiv \alpha^M(x_i)$, can be thought of as a sum of the SUT slopes, α_i^0, and contributions of random noise, α_i^R, error due to the drifts of the instrument and set-up, α_i^D, periodic temporal error uncorrelated with x_i and the measured slope, α_i^P, and systematic error of the measurement, α_i^S:

$$\alpha_i^M = \alpha_i^0 + \alpha_i^R + \alpha_i^D + \alpha_i^P + \alpha_i^S . \quad (1)$$

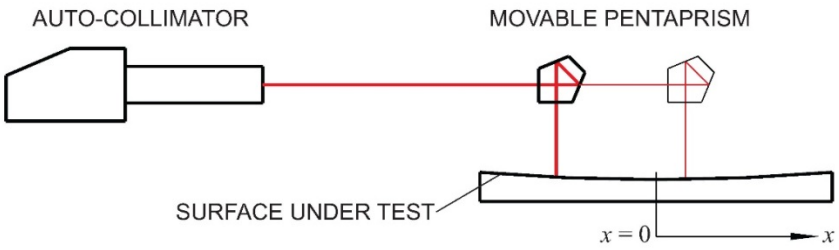

Figure 1: Simplified schematic of experimental arrangement for surface slope profiling with a deflectometer based on an auto-collimator as an angular sensor and a movable pentaprism for scanning the sample beam along the surface under test. The pentaprism is shown in two different positions.

Accurate measurement of α_i^0 assumes insignificant contributions of random noise, temporal errors (due to drifts and spurious periodic fluctuations), and systematic errors. Below, we briefly analyze the major sources of the errors in slope profilometry.

2.1 Random error

The main source of random error in the surface profilometry is air convection (turbulence) along the optical path, as caused by temperature gradients and air flow.[58] Due to air convection the refractive index of the air along the optical path changes, leading to pointing instability of the light beam. The air-convection error can be suppressed by shielding the optical path. However, application of adequate shielding in a scanning profiler is difficult (if not impossible) because of its continuous coordinate change during a measurement (Fig. 1).

The intensity of the air convection, as well as the overall stability of an optical profiler system, are strongly correlated with environmental conditions in the lab. For this reason, the new ALS XROL[49,50] is constructed to keep the cleanroom laboratory at temperature of 20 ºC with a long term (over a few days) stability of about ±30 mK. Additional temperature insulation of each XROL instrument setup with surrounding hutch and curtain system, drops the temperature variation over the measuring setup to the level of a few mK. Nevertheless, the resulting random error of the slope reading with XROL slope profilers[15,22,57] is still rather large at about 0.2-0.3 μrad/Hz$^{1/2}$. This can also be the result of the unavoidable air flow from each instrument's carriage air-bearing system.

The air convection noise has a low frequency characteristic with typical frequencies of 0.1-1 Hz.[58] For efficient suppression of the noise by averaging the repeated measurements, the interval between the measurements has to be much larger than 10 sec. In Sec. 3, we show that suppression of the instrumental drift and systematic errors can be achieved by averaging multiple measurements performed under controlled changes of parameters of the experimental set-up and scanning (the direction of scanning, orientation, and alignment of the SUT, etc.). In this case, the low frequency random noise, as well as its fast component, is also effectively averaged out.

2.2 Drift errors

In order to be classified as a drift error, the temporal variation of the measurand has to be smooth and slow compared to the duration of the measurement scan. The error due to a drift is, in some sense, in-between the random noise and systematic error. In the general case, the contribution of the drift error cannot be averaged out using a number of scans identically carried out over a reasonable time. In contrast with systematic errors, drifts are usually not stable enough for a precise calibration.

The main sources of drift error in any physical measurement are slow variations of the environmental conditions (temperature, and air pressure and humidity in the lab) and inherent temporal instabilities of the measurement setup (for example, mechanical instability of the mirror mounting and alignment).

An experimental method for effective suppression of spurious effects in slope metrology caused by an instrument's slow measurement rate and setup drifts was suggested and first demonstrated in Ref.[53] According to the method, the slope profile measured in a single run is an average of surface slope traces recorded in an optimally arranged set of sequential scans with the profiler in the forward (F) and backward (B) directions (see Sec. 3 for more detailed discussion).

2.3 Temporal periodic errors uncorrelated with the measurement arrangement

A special case of the measurement error dependent on time, relates to the temporal periodic variation of the lab environmental conditions such as air temperature and pressure oscillation due to the operation mode of the lab air-conditioner. Thus, the ALS XROL cleanroom's temperature, measured with three temperature sensors mounted at different positions on the lab walls, has ~ 5-min periodic oscillation with peak-to-valley variation below ± 30 mK. The oscillation was found to be unavoidable due to an operation peculiarity of the computer control feedback system of the lab air-conditioner. Due to the double insulation of the lab instruments with the hutches and curtain systems, this oscillation appears to not affect high sensitivity metrology with our surface slope measuring profilers, LTP-II, DLTP, and OSMS, which are extremely sensitive to temperature instabilities and gradients around the measuring set-up.

Specific to the surface profilers utilizing air-bearing translation stages is the error associated with periodic variation of compressed air supplied to the stage air bearings. In the case of the ALS XROL, the DLTP stability tests[50,59] have depicted a strong correlation between the AC measurements of the carriage pitch angle and the pressure variation of the compressed air with a period of about 4.5 min. The rms variation of the pitch angle was found to be ~0.3 μrad. The variation of the yaw angle (the most important for the performance of the DLTP designed to measure side facing SUTs[59]) was smaller, < 0.1 μrad rms. A similar pitch angular variation was observed with the SPring-8 LTP.[18]

A known way to reduce the air-bearing pressure variation is to use a large volume reservoir tank in line with the high pressure airline supplied the air bearings and to optimize the flow rate of air coming to the tank with an input valve.[18,50] In our case, suppression of the air-bearing pressure variation by a factor of ~ 200 is possible due to the additional relatively large volume (estimated to be about 20-30 liters) of the pipes connecting the reservoir tank (200 liters) with the profiler's carriages.[50]

Generally, the error due to the periodic temporal pressure and temperature variations do not correlate with the measurement arrangement, such as the SUT shape and/or position along the measured trace, and therefore, cannot be treated as a systematic error. In order to suppress this error, we apply an original procedure consisting of a special arrangement of a delay time between sequential scans of the same measurement run. In Sec. 4, we discuss the procedure in more detail.

2.4 Systematic errors

As pointed out above, the major limiting factors of modern surface metrology systems are systematic errors, which are systematically reproduced in identical measurements (scans) and, therefore, cannot be suppressed by averaging over repeated measurements performed with an unchanged experimental arrangement. In an optical system, the most common sources of the systematic error are aberrations and material imperfections of the system's optical elements, imperfections of the sensor translation (for example, carriage wobbling), limited quality of the light detectors, etc. Due to the inherent repeatability of the systematic error, it can be calibrated out via the dedicated test measurements.

For surface slope profilers, a number of calibration methods were suggested (see, for example, Refs.[45,54,60-62] and references therein). However, due to the strong dependence of the systematic errors on a particular measurement arrangement including the specifics of the SUT surface shape and size, thorough calibration (useful for all potential experimental arrangements and SUT's shapes) is extremely difficult, if not impossible.

The drawback of the dependence of the systematic errors on the specific measurement arrangement can be advantageous if people use the correlation methods for suppression of systematic errors of slope profilers, as suggested in Ref.[51,52,55] (see also Sec. 6).

3. OPTIMAL SCANING STRATEGY METHOD FOR SUPPRESSION OF DRIFT ERROR AND RANDOM NOISE

3.1 One dimensional surface slope profiling

In the experimental method for the effective suppression of the instrumental and setup drifts,[53] a slope trace measurement run consists of a number of repeatable scans arranged with a sequential reversal of the direction of scanning towards increasing (forward, *F*) or decreasing (backward, *B*) in X_i and with an optional reversal of the orientation of the SUT with respect to the slope profiler. Such a run provides repeatable measurements at a certain point,

x_i, in a sequence of time moments, $t_i(s)$, where s is the scan number ($s = 1, 2, ..., S$, where S is the total number of scans in a single measurement run), specially arranged according to optimal scanning strategies analytically derived in Ref.[53] to anti-correlate the temporal dependence of the drift.

Mathematically, a sequence of scan directions in a measurement run is described with a binary sequence $\{r_s\}$ with the elements:

$$r_s = \begin{cases} F \text{ or } +1, & \text{if the s-th scan is performed in the forward direction,} \\ B \text{ or } -1, & \text{if the s-th scan is performed in the backward direction.} \end{cases} \tag{2}$$

An optimal strategy has to satisfy the correlation identity

$$\sum_{s=1}^{S=2^p} r_s \, s^{p-1} \equiv 0 \tag{3}$$

proven in Ref.[53] In Eq. (3) p is the order of the highest polynomial term in the drift function's MacLaurin series, which is suppressed using the scanning pattern given $\{r_s(p)\}$, including the lower orders. Obviously, the optimal scanning strategies, suitable for suppression of a linear drift, are:

$$r_s(1) = \{F, B\} \equiv \{+1, -1\} \quad \text{and} \quad r_s(1) = \{B, F\} \equiv \{-1, +1\}. \tag{4}$$

As shown in Ref.,[53] suppression of drifts of the second order would require a run consisting of 4 scans

$$r_s(2) = \{+1, -1, -1, +1\} \quad \text{or} \quad r_s(2) = \{-1, +1, +1, -1\}, \tag{5}$$

and for third order,

$$r_s(3) = \{+1, -1, -1, +1, -1, +1, +1, -1\} \quad \text{or} \quad r_s(3) = \{-1, +1, +1, -1, +1, -1, -1, +1\}, \tag{6}$$

Solutions (4-6) suggest that the suppression of any order drift automatically suppresses those of lower orders.

There is no apparent preferred directionality of the scans, so it is natural that if the set $\{r_s(p)\}$ is a solution then the set $\{-r_s(p)\}$ is also a solution [as depicted with Eqs. (4-6)]. Denoting the positive solution (started from the forward direction scan) for the p-th order drift suppression as $\{r_s^+(p)\}$ and the negative solution (started from the backward direction scan) as $\{r_s^-(p)\}$, the general recursion relation[53] between the sets $\{r_s^\pm(p+1)\}$ and $\{r_s^\pm(p)\}$ is

$$\{r_s^\pm(p+1)\} = \pm\{r_s^+(p), r_s^-(p)\}. \tag{7}$$

For the case when only the scanning direction is reversed, the corresponding suppression factor can be estimated[53] as a ratio of P-V variations of the major terms of the drift error of the optimized and non-optimized runs of the same total number of scans:

$$\xi \cong 8 \cdot 2^p / p. \tag{8}$$

Estimation (7) shows that suppression factor, ξ, rapidly increases with increase of p for $p \geq 2$. For the optimal strategy of eight scans, $\xi \approx 21$.

This is the simplest possible realization of the OSS method that we routinely use at the ALS XROL. Application of the OSS method to scanning profiler measurements also allows more effective suppression of low frequency random noise due to air convection because of the increased time between sequential expositions of a particular SUT point in different scans.

In Ref.,[53] also considered is a more sophisticated realization of the OSS method involving simultaneous reversals of both the scanning direction and the SUT orientation. In this case, the drift errors up to the certain polynomial order, determined by the OSS in use, can be absolutely zeroed (eliminated). The optimal scanning strategies that realize the drift error elimination are the same as those described with Eqs. (4-7). They consist of the equal numbers of the scans performed with the SUT in two opposite orientations. Averaging over the scans effectively eliminates the even part of the instrumental systematic error (see Sec. 5.1).

3.2 Two dimensional tracing

Extension of the optimal scanning strategy suggested in the recent publication[57] allows automatic suppression of the drift error in two-dimensional surface slope measurements using the 2D spatial translation of the gantry system, such as the one of the XROL OSMS. In this case (see Fig. 2), a measurement run to get a 2D slope map consists of a number of repeatable 2D scans in the forward (Fig. 2a) and the backward (Fig. 2b) direction, optimally arranged according to the prescription given in Sec. 3.1 with Eqs. (4-7).

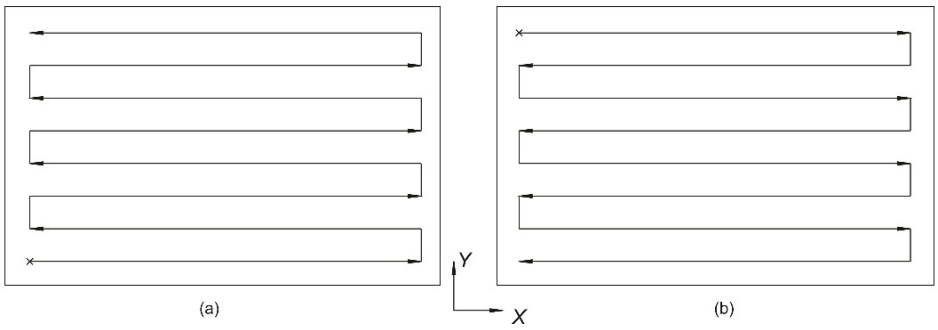

Figure 2: (a) 2D scan in the forward and (b) in the backward direction. The 2D scans starting from tracing in X-direction are shown. A similar definition of the forward and backward scans can be applied to 2D scans that start from the measurement in Y-direction. The crosses depict the starting points of the scans.

4. SUPPRESSION OF PERIODIC ERRORS

We consider here the error of the surface slope measurements, $\alpha^P(t)$, due to a time dependent periodic perturbation with characteristic time of variation significantly shorter than the duration of a single measurement scan, T. Being periodic and fast, the error cannot be treated as the random noise or drift error. We also assume that $\alpha^P(t)$ is well insulated from the measurement arrangement, meaning that the error does not correlate to (is not a function of) the SUT slope angle α_i^0 and/or position x_i along the SUT (as is the case of the systematic error).

In order to effectively reduce the periodic perturbation impact on measurement, we suggest and discuss here adding a time delay between successive scans so that upon averaging, the periodic error is cancelled, or, at least, significantly suppressed.

4.1 Error due to a harmonic temporal perturbation in the optimal two-scan run

Let us consider the case of the periodic error described by a harmonic function:

$$\alpha^P(t) = A\sin(t\,2\pi/\tau + \varphi_0), \tag{9}$$

where A and τ are the error amplitude and period of the perturbation, respectively, $t = 0$ corresponds to the moment of start of the measurement, and φ_0 is the perturbation phase at $t = 0$.

The error contribution to the first scan performed in the forward direction can be expressed as

$$\alpha_1^P(t) = A\sin(t\,2\pi/\tau + \varphi_0), \quad 0 \le t \le T. \tag{10}$$

In Eq. (10), the subscript index '1' denotes the scan number, in this case $s=1$.

With a time delay δt introduced between the scans and described with an additional phase $\theta = \delta t\, 2\pi/\tau$, the error contribution to the second scan performed in the backward direction is

$$\alpha_2^P(t) = A\sin([T-t]2\pi/\tau + T\,2\pi/\tau + \varphi_0 + \theta), \quad 0 \le t \le T; \tag{11}$$

here, the running time t is matched to the position on the SUT surface. The resulted error is [compare with Eq. (1)]:

$$\alpha_i^P = \frac{\alpha_{2,i}^P + \alpha_{1,i}^P}{2} = \frac{A}{2}\left[-\sin(i\,\Delta t\, 2\pi/\tau - T\,4\pi/\tau - \varphi_0 - \theta) + \sin(i\,\Delta t\, 2\pi/\tau + \varphi_0)\right], \tag{12}$$

where Δt is the time increment between two sequential measurement points, $i = [0,1,...,I]$, $T = I\,\Delta t$.

In order to zero the error (12) contained in the average of two scans in the forward and backward directions, one needs to correlate the delay time δt with the initial phase φ_0 and the one scan duration T to get an integer number n of periods of the perturbation τ:

$$4\pi T/\tau + 2\varphi_0 + \theta = 2n\pi. \tag{13}$$

Therefore, besides τ and T, one should also know the initial phase φ_0. The later requirements can be fulfilled if the profiler is designed with a capability to continuously monitor the perturbation; so that the first scan is always started at a certain φ_0, for example, at $\varphi_0 = 0$. Then, Eq. (13) gives the condition to the value of the delay time between the scans:

$$0 < \delta t = n\tau - 2T. \tag{14}$$

4.2 Error due to a harmonic temporal perturbation in the optimal four-scan run

In the notations above, the error contributions to the third backward and the fourth forward scans are, respectively,

$$\alpha_3^P(t) = A\sin([T-t]2\pi/\tau + 2T\,2\pi/\tau + \varphi_0 + 2\theta), \quad 0 \le t \le T; \tag{15}$$

$$\alpha_4^P(t) = A\sin(t\,2\pi/\tau + 3T\,2\pi/\tau + \varphi_0 + 3\theta), \quad 0 \le t \le T. \tag{16}$$

Due to the additional scans, there is a possibility to completely zero the harmonic error in the average of the 1st and 4th scans and the 2nd and 3rd scans:

$$\frac{\alpha_{4,i}^P + \alpha_{1,i}^P}{2} = \frac{A}{2}\left[\sin(i\,\Delta t\, 2\pi/\tau + 3T\,2\pi/\tau + \varphi_0 + 3\theta) + \sin(i\,\Delta t\, 2\pi/\tau + \varphi_0)\right] \text{ and} \tag{17}$$

$$\frac{\alpha_{3,i}^P + \alpha_{2,i}^P}{2} = -\frac{A}{2}\left[\sin(i\,\Delta t\, 2\pi/\tau - 3T\,2\pi/\tau - \varphi_0 - 2\theta) + \sin(i\,\Delta t\, 2\pi/\tau - 2T\,2\pi/\tau - \varphi_0 - \theta)\right], \tag{18}$$

if we select the delay between the scans δt to be:

$$0 < \delta t = \tau\,(2k+1)/2 - T \text{ , where } k \text{ is a natural number.} \tag{19}$$

Figure 3a illustrates the complete illumination of a temporal harmonic error in the result of four optimally arranged scans with a delay time between the scans given by Eq. (19). Here, $T = 40$ min, $\tau = 4.8$ min, and $k = 8$. The delay time $\delta t = 0.8$ min does not depend on the value of the initial phase, selected in Fig. 3a to be $\varphi_0 = \pi/3.7$.

4.3 Suppression of the error due to a periodic or a quasi-periodic temporal perturbation

A similar procedure, as the one considered in Sec. 4.2, is applicable for the suppression of errors associated with a periodic (but non-harmonic), or even quasi-periodic temporal perturbations. In this case, the clue to the selection of the optimal delay time is the period corresponding to the maximum intensity peak in the power spectral density of the

perturbation signal. Using this period in (19), one can find the delay time providing a partial suppression of the error. This approach closely relates to the correlation method for suppression of the systematic error[55] (see Sec. 5.2). Its efficacy is illustrated with the simulations depicted in Fig. 3b, where the quasi-periodic temporal error with the rms variation of 347 nrad corresponds to the pressure variation of the compressed air supplied to the DLTP air-bearing system. In order to find the optimal delay time with Eq. (19), we first determine the effective period from the perturbation autocorrelation function. The resulted contribution of the error to the average of 4 scans [Fig. 3(b1)] has the rms variation of 132 nrad.

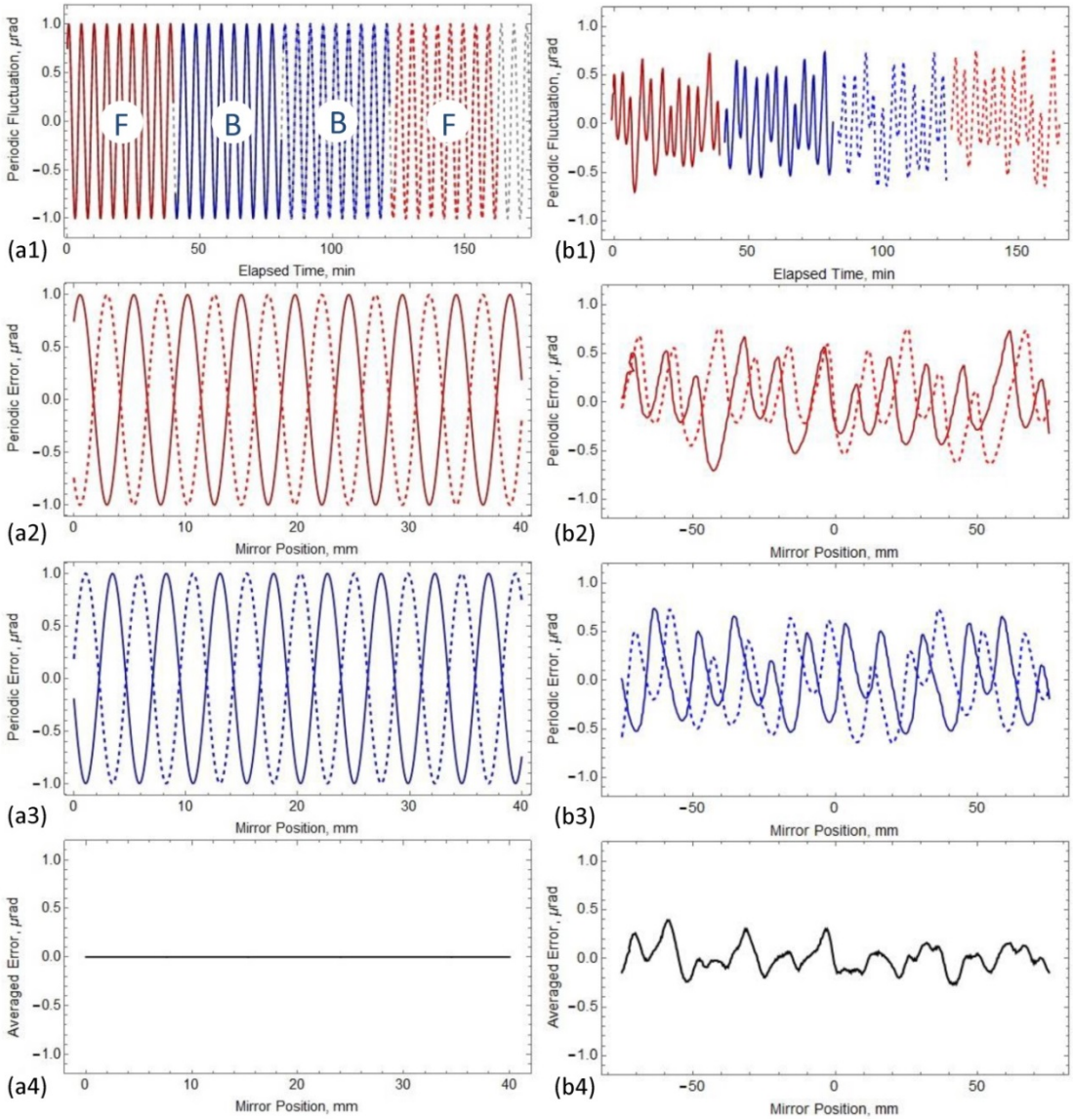

Figure 3: (a) Illumination of a temporal harmonic error with the period of 4.8 min in the result of four optimally arranged scans (a1) with the duration of 40 min each. The optimal delay time of 0.8 min allows compensating the contribution of the temporal harmonic perturbation to the average of (a2) the forward and (a3) the backward scans, respectively. The total error (a4) is completely averaged out independently on the value of the initial phase of the error. (b) Suppression of a temporal quasi-periodic error corresponding to the pressure variation of the compressed air supplied to the DLTP air-bearing system. The simulations were performed for the same arrangement of the scans as in the case (a). (b2) and (b3) The contribution of the errors to the forward and the backward scans, respectively. The rms variation of the resulted error in (a4) is 132 nrad.

An additional suppression of periodic or a quasi-periodic error is possible by optimal selection of the delay time(s) in the 8-scan OSS run. A more detailed discussion of these possibilities is beyond the scope of the present paper.

5. CORRELATION METHODS FOR SUPPRESSION OF SYSTEMATIC ERRORS

The systematic errors of a slope profiler can be divided into two groups, as distinguished by the spatial frequency range at which they perturb. One group relates to the uncertainty of the instrumental calibration, corresponding to relatively lower spatial frequencies. Such errors appear, for example, due to aberration of the profiler's Fourier transform lens or an out-of-focus position of the CCD detector, and can be relatively easy to calibrate with a dedicated tilting stage.[42,43,45,46,54]

The other group of systematic errors relates to the quality of the instrument's optical elements, and contributes to the error at relatively higher spatial frequencies. These include the systematic errors due to optical inhomogeneity of materials used in the profiler's optical elements, the quality of the reflecting surfaces, and the components of the CCD detector system, etc.[21-26,63-65] In the measured slope trace, these systematic errors appear as local (relatively high spatial frequency) perturbations with amplitudes up to 1 μrad and larger. Because these systematic errors strongly depend on the peculiarities of the SUT and the experimental arrangement, it is very difficult to account for such errors via precision calibration.

Besides using direct calibration, one can make repeat measurements with different experimental arrangements with the goal of decreasing the systematic error in the averaged result. The simplest method of this kind is that of reduction of systematic error with a certain symmetry with respect to reversing (flipping) the SUT by 180 degrees around its tangential center.[51,52]

Additionally, one can perform multiple measurements with the same SUT orientation, but with different arrangements (pitch and roll tilts, lateral position, and orientations) with respect to the instrument's optics and detector.[55,66] For an optimal set of measurements, the systematic perturbation would appear at different locations along the slope traces and could be reduced by averaging over the measurements.

Such correlation methods are briefly discussed in Secs. 5.1 and 5.2.

5.1 Reduction of the even part of the systematic errors in surface slope metrology by flipping of SUT

A method for reducing systematic errors with a certain symmetry in measurements with a surface slope profiler was introduced by McKinney and Irick.[51,52] The method is based upon decomposing the systematic error signal into odd and even functions. Two sets of measurements are made along the same line on the SUT, the second after reversing the SUT by rotating (flipping) by 180 degrees.

In Ref.,[63] it is pointed out that mathematical manipulation of two data sets allows one to effectively correct for the even or odd part of the error signal. Really, only the even part of the systematic error of slope measurements can be compensated this way. Because of the possible confusion, the flipping method is briefly reviewed below.

Without loss of generality, we assume here that the coordinate system of the deflectometer originates at the center of the SUT clear aperture; the direction of the x-axis is defined with respect to the profiler (Fig. 1), rather than to the SUT that is a subject for flipping.

Let us decompose the systematic error of a measurement $\alpha^S(x)$ to two functions with different inverse symmetry:

$$\alpha^S(x) = \alpha^S_{EVEN}(x) + \alpha^S_{ODD}(x), \tag{20}$$

where the functions $f_{EVEN}(x)$ and $f_{ODD}(x)$ are, respectively, even and odd with respect to the inversion of the variable x:

$$\alpha^S_{EVEN}(-x) = \alpha^S_{EVEN}(x) \quad \text{and} \quad \alpha^S_{ODD}(-x) = -\alpha^S_{ODD}(x). \tag{21}$$

Such decomposition exists for any smooth function $\alpha^S(x)$ that can be represented, for example, with Taylor or Fourier series.

A surface slope measurement performed with the direct orientation of the SUT can be written as

$$\alpha^M_D(x) = \alpha^0(x) + \alpha^S_{EVEN}(x) + \alpha^S_{ODD}(x); \tag{22}$$

whereas, a measurement with the SUT flipped around its center given by $x=0$ is described with

$$\alpha_F^M(x) = -\alpha^0(-x) + \alpha_{EVEN}^S(x) + \alpha_{ODD}^S(x). \tag{23}$$

In order to average the measurements (22) and (23), one should transform Eq. (23) to the coordinate system related to the SUT surface by inverting the coordinate: $x \to -x$, and the sign of the measured slope values: $\alpha_F^M \to -\alpha_F^M$:

$$-\alpha_F^M(-x) = \alpha^0(x) - \alpha_{EVEN}^S(x) + \alpha_{ODD}^S(x). \tag{24}$$

In Eq. (24), we accounted for the symmetry properties of the systematic error functions given by Eq. (21).

Finally, the average of the measurements (4) and (6) is

$$\alpha_{AVR}^M(x) = \frac{\alpha_D^M(x) - \alpha_F^M(-x)}{2} = \alpha^0(x) + \alpha_{ODD}^S(x). \tag{25}$$

Analogously, half of the difference of the measurements is

$$\alpha_{DIF}^M(x) = \frac{\alpha_D^M(x) + \alpha_F^M(-x)}{2} = \alpha_{EVEN}^S(x). \tag{26}$$

Therefore, the half difference provides the even part of the instrumental systematic error eliminated by averaging the measurements performed with the SUT placed in the direct and in the flipped orientations with respect to the instrumental coordinate system.

So far, we consider the systematic error that is a function of the position coordinate x and does not depend on the value of the surface slope. However, in the surface slope profilometry with significantly curved mirrors, a more common systematic error is the one that is a function of the surface slope angle:

$$\alpha_D^M(x) = \alpha^0(x) + \alpha^S(\alpha^0(x)). \tag{27}$$

Using decomposition analogous to Eq. (21) but now in the angular domain,

$$\alpha_{EVEN}^S(-\alpha^0(x)) = \alpha_{EVEN}^S(\alpha^0(x)) \quad \text{and} \quad \alpha_{ODD}^S(-\alpha^0(x)) = -\alpha_{ODD}^S(\alpha^0(x)), \tag{28}$$

we can write the slope traces measured with the mirror with the direct and flipped orientations as

$$\alpha_D^M(x) = \alpha^0(x) + \alpha_{EVEN}^S(\alpha^0(x)) + \alpha_{ODD}^S(\alpha^0(x)), \text{ and} \tag{29}$$

$$\alpha_F^M(x) = -\alpha^0(-x) + \alpha_{EVEN}^S(-\alpha^0(-x)) + \alpha_{ODD}^S(-\alpha^0(-x)). \tag{30}$$

Transformation of Eq. (30) back to the coordinate system related to the SUT surface by inverting the coordinate: $x \to -x$, and the sign of the measured slope values: $\alpha_F^M \to -\alpha_F^M$ gives

$$-\alpha_F^M(-x) = \alpha^0(x) - \alpha_{EVEN}^S(-\alpha^0(x)) - \alpha_{ODD}^S(-\alpha^0(x)), \text{ or} \tag{31}$$

$$-\alpha_F^M(-x) = \alpha^0(x) - \alpha_{EVEN}^S(\alpha^0(x)) + \alpha_{ODD}^S(\alpha^0(x)). \tag{32}$$

Analogously to the results in Eqs. (25) and (26), the average of the direct (29) and flipped (32) measurements is free of the even part of the systematic error:

$$\alpha_{AVR}^M(x) = \alpha^0(x) + \alpha_{ODD}^S(\alpha^0(x)); \tag{33}$$

whereas, the half of the difference of the measurements contains only the even part of the systematic error:

$$\alpha^{M}_{DIF}(x) = \alpha^{S}_{EVEN}(\alpha^{0}(x)). \tag{34}$$

It is a common practice to estimate the rest of the systematic error in the averaged result, $\alpha^{S}_{ODD}(x)$ and $\alpha^{S}_{ODD}(\alpha^{0}(x))$, with the rms (or peak-to-valley) variation of the removed systematic error, $\alpha^{S}_{EVEN}(x)$ and $\alpha^{S}_{EVEN}(\alpha^{0}(x))$ found from the difference of the measurements with the mirror in the direct and flipped orientations. This approach is mathematically incorrect. However, we often do not have a better method and argue (also without a strong mathematical motive) that for a reasonably smooth systematic error function, the estimation is valid.

5.2 Correlation analysis for randomization of systematic errors dependent on the lateral position and/or the measured slope value

The SUT flipping method discussed in Sec. 5.1 can be thought of as a method utilizing the property of strong anti-correlation between contributions of the even part of the systematic error to the measurement performed with the SUT in two opposite orientations. Due to the anti-correlation, the even part of the systematic error is removed from the average of the measurements.

Really, the same idea of finding and exploiting experimental arrangements with anti-correlating errors is in the foundation of the OSS method[53,57] (Sec. 3) and the method for suppression of the periodic and quasi-periodic temporal errors, both independent on the SUT shape and measurement arrangement (Sec. 4).

In this section, we briefly review the results of Refs.[55,66] on applying the correlation analysis technique for randomization of instrumental systematic errors directly dependent on the peculiarities of the measurement such as the lateral position along the SUT and the SUT shape (slope variation). The idea is still the same: to arrange repeatable measurements in a manner suitable for suppression of the systematic error contribution to the averaged result.

Consider a systematic effect, described with a function $\alpha^{S}(x)$ of a single variable x (Fig. 1). Ignoring other terms depicted in Eq. (1), a contribution of the systematic error to a measurement $\alpha^{M}(x)$ of the SUT slope trace $\alpha^{0}(x)$ is

$$\alpha^{M}_{l=0}(x) = \alpha^{0}(x) + \alpha^{S}(x). \tag{35}$$

In order to reduce the contribution of the systematic error, the measurement is repeated with the SUT shifted in the tangential direction by some distance l that changes the SUT lateral position with respect to the optical sensor (the AC in Fig. 1) but does not change the SUT slope variation in the mirror-related coordinate system:

$$\alpha^{M}_{l=l_1}(x) = \alpha^{0}(x) + \alpha^{S}(x + l_1). \tag{36}$$

The shift value is selected[55] to minimize the rms contribution of the systematic error to the average of these two measurements:

$$\alpha^{AVR}(x) = \alpha^{0}(x) + \frac{\alpha^{S}(x) + \alpha^{S}(x + l_1)}{2}, \tag{37}$$

and is equal to the position (lag) of the strongest negative (anti-correlation) peaks of the auto-correlation function $AC(l)$ of the systematic error, such that

$$l_1 = \arg\min AC(l), \tag{38}$$

where the function $\arg\min f(t)$ gives the value of $t_{\min}$ for which the function reaches its minimum.

The consideration above can be straightforwardly applied to the case of the systematic error dependent on the measured slope value. In this case, the second repeated measurement is performed with the SUT pitch tilted by the angle that corresponds to the minima of the systematic error auto-correlation function in the slope domain. The corresponding values of the SUT shift (tilt) values, optimal for suppression of the systematic error, can be determined based, for example, on the correlation analysis of the preliminary measured profiler's calibration[46] or the first test measurement with the SUT.

Averaging over two measurements with a single pitch tilt between them has been suggested, implemented, and proven to be highly effective for suppression of systematic periodic oscillation in slope measurements with an autocollimator-based slope profiler.[22,23] In the case of the ALS DLTP[22] and the OSMS,[57] the major AC systematic oscillation is at the angular period of approximately 280 μrad. In order to suppress the error, we routinely perform a repeated measurement after 140-μrad relative tilt of the SUT. The method was also successfully applied to suppression of the systematic error of an AC used for calibration of the ALS LTP-II.[46]

A generalization of the method to the case of a few strong minima in the systematic error auto-correlation function is considered in Ref.[55] In this case, additional repeatable measurements are performed with the lateral shifts and/or pitch tilts corresponding to the found minima of the auto-correlation function.

6. ADVANCED OPTIMAL SCANNING STRATEGY TECHNIQUE

All the methods for suppression of the measurement errors considered above are based on averaging multiple measurements specially arranged to minimize the contribution of the errors in the final result. In our lab, in order to suppress the random and drift error, a single run usually consists of 8 scans performed according to the optimal sequence given by Eq. (6). In order to suppress the known periodic systematic error of the auto-collimator, we perform one more run with the SUT with the additional pitch tilt of ~140 μrad. Next, in order to suppress the even part of the systematic error, we carry out two more runs with the flipped SUT again with the relative pitch tilt of 140 μrad. Therefore, the minimum number of runs is four. This does not include the test measurements needed in the case if there is a characteristic variation in the measured slope trace that cannot be *a priory* assigned to the SUT or to the instrumental systematic error.

Here, we consider a manner in which all these repeatable tests can be arranged into a single run of 8 scans providing a significant, by a factor of 4, increase of the measurement rate at no degradation of the accuracy of the surface slope metrology.

6.1 Optimal scanning strategies in the terms of optimal square waveforms

In Sec. 3.1 we mentioned that the OSS based drift suppression becomes absolute when scans with simultaneous reversals of the scanning direction and the SUT orientation are made.[53] The optimal scanning strategies that realize the drift error elimination are the same as ones described with Eqs. (4-7) and derived in Ref.[53] They consist of the equal numbers of the scans performed with the SUT in opposite orientations. At first glance, this is an optimal strategy to effectively eliminate the drift error and the even part of the instrumental error (see Sec. 5.1) without an increase of the total number of scans. However, it is not generally true.

The practical reason is based on the fact that any (automated or manual) change of the experimental arrangement is generally accompanied with a perturbation to the measurement environmental conditions. For example, a heat load in the course of flipping of the SUT with an automated rotation stage will change the surrounding temperature that, in its turn, can cause an additional drift error. In order to minimize this spurious cross-talk, the sequences of changes of the experimental parameters (in this case, the direction of scanning and the SUT orientation) should be mutually anti-correlated; or in other words, the sequences of changing the parameters have to be orthogonal.

Similar to the combined suppression of the drift and the even systematic errors, the same OSS should not be used for an additional suppression of the systematic errors associated, for example, with the overall shift and/or tilt of the SUT with respect to the profiler.

A solution to the problem of switching multiple experimental parameters is presented in Ref.,[67] where the optimal square waveforms for drift-free multichannel phase-sensitive detection are discussed. The derived optimal switching waveforms were first used in Refs.[68,69] in an experiment, searching for parity (P) and time reversal invariance (T) violating electric dipole moment (EDM) of xenon. Since then, this technique has been widely used in experiments searching for P and T violating EDMs in neutrons,[70-72] atoms,[73-75] molecules,[76-78] and solids.[79] Below, we apply the consideration based on the optimal square waveforms to derivation of the advanced optimal scanning strategies, suitable for the suppression, in a single run of the measurement, of random noise, drift error, the even part of the systematic errors, and the instrumental error, anti-correlated with the SUT lateral shift or pitch tilt (Sec. 5.2).

Figure 4a shows the square waveform S_{111} corresponding to the optimal scanning strategy of 8 scans $r_s^+(3)$ given by Eq. (6). In notation of Ref.,[67] the waveform S_{111} is a product of three waveforms:

$$S_{111} = S_{001} S_{010} S_{100}, \tag{39}$$

depicted in Fig. 4 as the periodic square waveforms (b), (c), and (d), respectively. The periodic square waveforms in Fig. 4 constitute the complete basis of periodic waveforms for the selected total number of scans of 8. Note that

$$(S_{001})^2 = (S_{010})^2 = (S_{100})^2 = 1. \tag{40}$$

Therefore, the total number of waveforms that can be generated as a product of the waveforms S_{001}, S_{010}, and S_{100} are (2^3-1)=7. The remaining three waveforms S_{011}, S_{110}, and S_{101} are shown in Fig. 5.

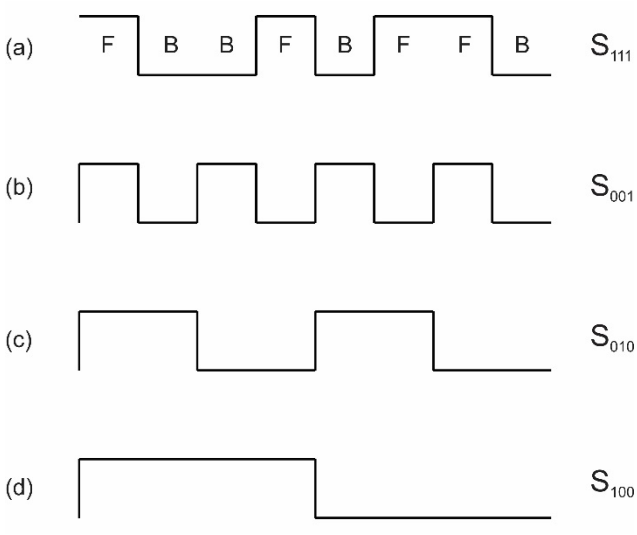

Figure 4: (a) Square waveform that corresponds to the OSS of 8 scans $r_s^+(3) = \{F, B, B, F, B, F, F, B\}$ given by Eq. (6). Plots (b), (c), and (d) are the periodic square waveforms that constitute the complete basis of periodic waveforms for the selected total number of scans of 8. The notation on the waveform corresponds to that of Ref.[67]

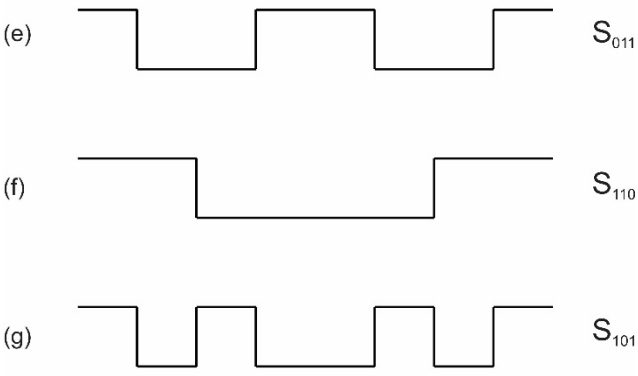

Figure 5: The remaining (with respect to the waveforms in Fig. 3) three waveforms S_{011}, S_{110}, and S_{101} obtained as the corresponding products of the basis waveforms S_{001}, S_{010}, and S_{100}.

6.2 Advanced optimal scanning strategies, AOSS

The seven waveforms shown in Figs. 3 and 4 are mutually orthogonal. That means that the sum of the element of the product of any two different waveforms is equal zero:

$$\sum_{s=1}^{S=8}\{S_a\, S_b\}_s = 0, \text{ if } a \neq b, \text{ and } \sum_{s=1}^{S=8}\{S_a\, S_b\}_s = S, \text{ if } a = b. \tag{41}$$

Among these waveforms, there are three that also satisfy the requirement to be the trend-free OSS: S_{111}, S_{110}, and S_{100} that corresponds to the OSS sequences: $r_s^+(3) = \{+1,-1,-1,+1,-1,+1,+1,-1\}$, $r_s^+(2) = \{+1,-1,-1,+1\}$, and $r_s^+(1) = \{+1,-1\}$, respectively. This set of optimal scanning strategies composites the advanced OSS, AOSS, that is optimal for sequential switching in the particular case of a single run of 8 scans the direction of scanning with S_{111}, the SUT pitch tilt (or lateral shift) with S_{110}, and the SUT orientation with S_{100}. The AOSS for larger number of switching parameters, and therefore, with correspondingly larger number of sequential scans, can be derived by using the prescriptions above.

Figure 6 illustrate suppression of the exponential instrumental drift in an 8-scan run arranged according to the AOSS composited of S_{111} sequence for switching the scanning direction and S_{100} sequence for flipping the SUT orientation.

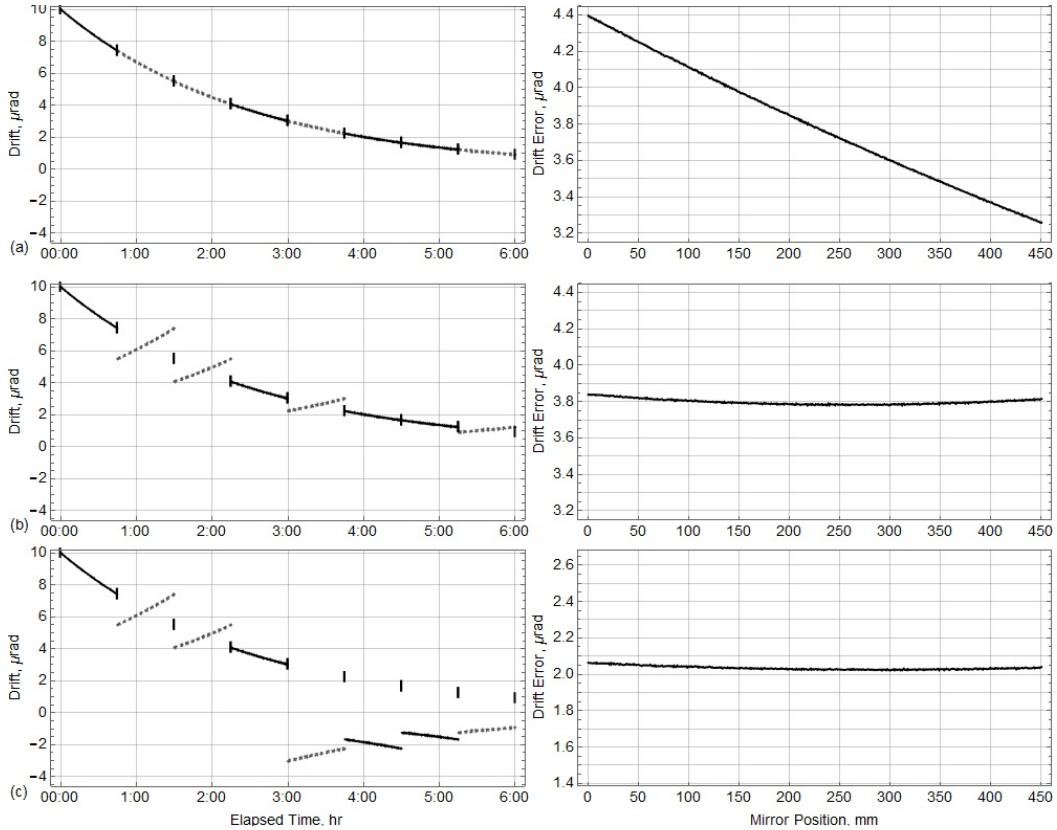

Figure 6: Illustration of drift error suppression with an AOSS technique. Contribution of the exponential drift in the slope trace measured in each scan of 8-scan run (the left-hand plot) and the corresponding drift error averaged over these 8 scans (the left hand plots): (a) all scans are performed in the forward direction with no flipping; (b) the scans are performed according to the OSS S_{111} with no flipping; and (c) the run is arranged according to an AOSS composited of S_{111} sequence for switching the scanning direction and S_{100} sequence for flipping the SUT orientation. See discussion in the text.

For the numerical simulations in Fig. 6, we consider an exponential temporal variation of the drift error with the decay time of 2.7 hours and the starting amplitude of 10 μrad. The duration of a single scan is 45 min. In the case of Fig. 6a of scanning in the forward direction only, the drift error averaged over all 8 scans has a strong, close to linear trend with the peak-to-valley variation of about 1.1 μrad and 0.33 μrad rms variation.

By arranging the measurement run according to the OSS S_{111} (with no flipping), the drift error is suppressed by a factor of ~20; see Fig. 6b. In this case, the resulted drift error is characterized with the P-V and rms variations of about 0.06 μrad and 0.015 μrad, respectively.

If the run is arranged according to an AOSS composited of S_{111} sequence for switching the scanning direction and S_{100} sequence for flipping the SUT orientation, the drift error is additionally suppressed by a factor of 1.5 to the P-V and rms variations of about 0.043 μrad and 0.010 μrad, respectively. Note that introduction of flipping of the SUT between the 4th and 5th scans leads to a significant decrease (by a factor of almost 2) of the angular offset due to the drift error contribution. Generally, the offset (that can be thought as an overall tilt of the SUT) does not compromise the surface slope measurements. However, it can potentially affect the high spatial frequency component of the instrumental systematic error.

7. APPLICATION OF THE ADVANCED OSS TECHNIQUE TO THE MEASUREMENTS WITH A HYPERBOLIC X-RAY MIRROR

7.1 Experimental set-up of the ALS Optical Surface Measuring System

A new Optical Surface Measuring System capable of 2D surface-slope metrology at an absolute accuracy below 50 nrad (in the slope domain) and < 1 nm (in the height domain) is under development at the ALS XROL. The gantry system has been specified, purchased, installed, and commissioned at the XROL in 2015-2016 (Fig. 7).

The key elements of the OSMS granite gantry system (that, in our case, is more appropriately named 'multifunctional translation system,' or MFTS) are the NOM-like 2D air-bearing translation system[19,20] and a custom-designed precision air-bearing stage for tilting and flipping the SUT.

(a)  (b) 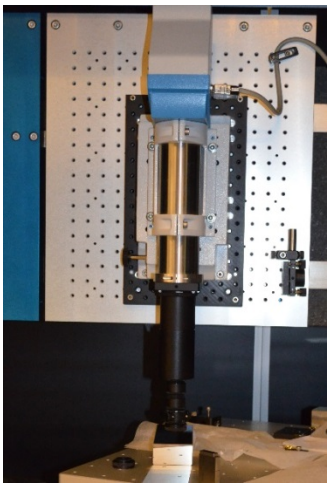

Figure 7: (a) The OSMS with the multifunctional translation system, MFTS, installed in the ALS XROL. (b) The OSMS slope mapping arrangement with an autocollimator vertically mounted on the OSMS MFTS carriage and used as a sensor.

The 2D air-bearing translation system allows automatically controlled scanning of the sensor optical head across the SUT in two orthogonal directions. In addition to these two translations, the OSMS MFTS has a precise tilting/flipping stage capable for automatically controlled tilting and rotation of the SUT in the course of a measurement run, as well as vertical (*Z*-axis) shifting of the SUT. These additional translations are crucial for implementation of experimental methods to automatically suppress the errors in a measurement run via optimal arrangement of repeatable scans discussed above in Secs. 3-6.

The OSMS MFTS was custom designed and fabricated by Q-Sys Company.[80] All of the motion controls and data acquisition systems are based on the NI LabView™ platform. More information on the design, specification, and performance of the OSMS MFTS can be found in Refs.[41,44,57]

7.2 Application of the AOSS technique to slope measurements with a high quality hyperbolic x-ray mirror

The ALS OSMS, equipped with an autocollimator directly mounted to the carriage in the vertical orientation (Fig. 7b), was used for 2D slope metrology with a hyperbolic cylinder x-ray mirror developed for the ALS QERLIN beamline.[81] The goal of the measurements was to firstly test the efficiency of the AOSS technique in application to the 2D surface slope mapping over the mirror clear aperture.

The mirror substrate with overall dimensions of 160 × 50 × 50 mm^3 and CA of 150 × 20 mm^2 are made of gold coated single crystal <100> silicon. The hyperbolic cylinder shape of the mirror is specified in the terms of the mirror beamline application (conjugate) parameters R_1, R_2, and θ, where R_1=700 mm is the distance between the object to hyperbolic mirror center, R_2=1781.97 mm is the distance from the second (virtual) focus to the center of the hyperbolic mirror, and θ=2.0 degrees is the grazing incidence angle at the mirror center. The overall tangential slope variation is about 2 mrad. The surface slope error along two tangential traces shifted by ± 5 mm from the mirror sagittal center is specified to be < 250 nrad (rms). The 2D mapping performed in a single run of 8 scans included three tangential traces, the two specified shifted traces and the one trace along the sagittal center, measured with the increment of 0.2 mm. The total duration of a single run was about 36 hours.

The major spurious effects expected are the major known systematic error of the AC with the period of about 280-290 μrad and the pitch wobbling of the X- and Y-translations of the carriage and the slab, respectively. With the auto-collimator mounted directly to the carriage, the measurements are most sensitive to the both wobbling effects. Partially, these errors have to be corrected by averaging the additional measurements with tilting and flipping the SUT. Therefore, a single 8-scan run was arranged according to the AOSS with switching the direction of scanning according to the strategy S_{111}, tilting the SUT pitch angle by ~140 μrad with S_{110}, and flipping the SUT orientation with S_{100}.

7.2.1 Suppression of the even part of the systematic error by changing the mirror orientation

Figure 8 depicts the result of the measurement along the center tangential line within the mirror clear aperture.

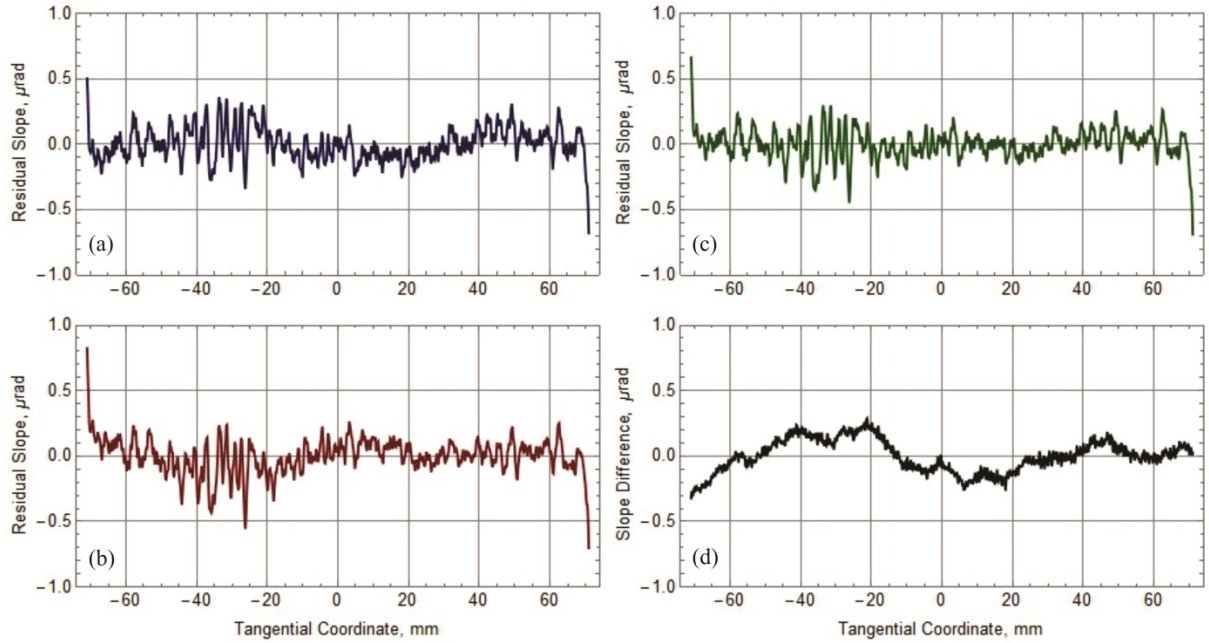

Figure 8: The result of the measurement along the center tangential line within the mirror clear aperture. (a) and (b): The residual (after subtraction of the desired hyperbolic shape) slope distributions averaged over 4 runs performed with the mirror in the direct and flipped orientation, respectively; (c) the resulted residual slope trace averaged over all 8 scans; and (d) the difference between the slope distributions measured with the mirror in the direct and flipped orientation.

Each residual (after subtraction of the desired hyperbolic shape) slope trace (with the increment of 0.2 mm) in Figs. 8a and 8b is the result of averaging over 4 scans performed with the mirror in the direct [plot (a)] and flipped orientation [plot (b)]. The resulted trace obtained by averaging of all 8 scans is shown in plot (c) of Fig. 8. The systematic error removed by flipping of the mirror is equal to a half of the difference (Fig. 8d) between the traces obtained with the mirror in the direct (Fig. 8a) and flipped (Fig. 8b) orientation. The rms variation of the removed error (the half difference) is only about 60 nrad. That suggests there was an extremely small contribution to the measurements of the gantry system's wobbling error.

7.2.2 Suppression of the AC periodic systematic error by tilting the mirror

Figure 9 demonstrates the efficacy of suppression of the AC periodic systematic error in the same run as in Fig. 8.

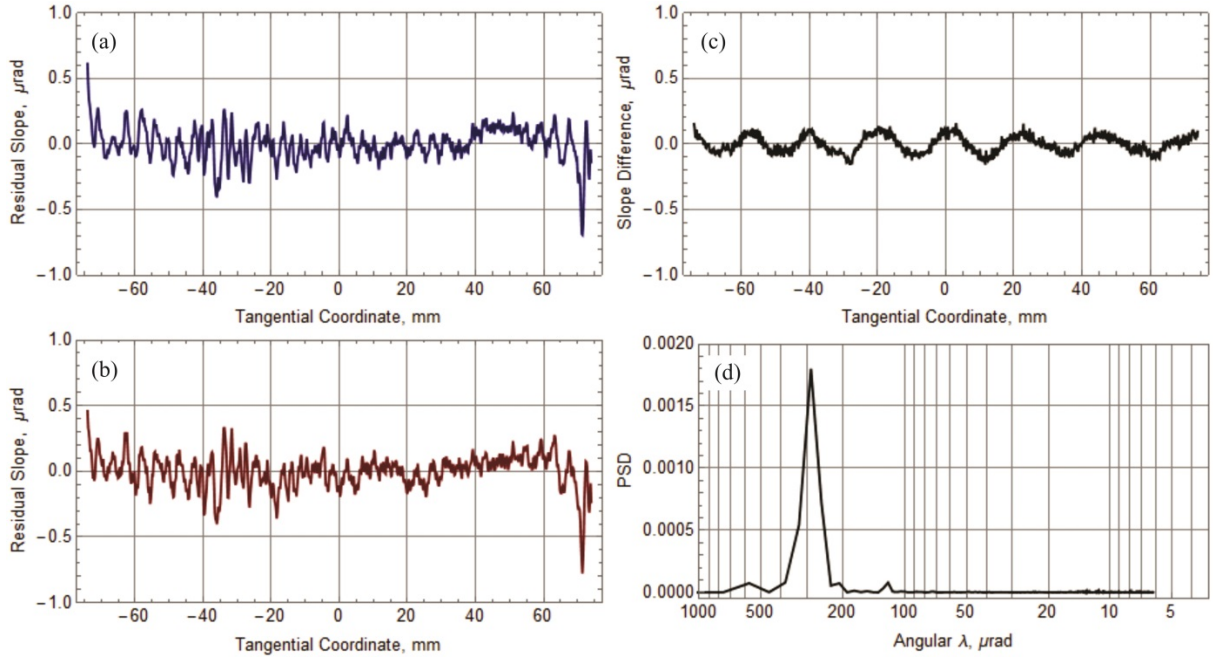

Figure 9: Suppression of the periodic systematic error of the AC. (a) and (b): The residual (after subtraction of the desired hyperbolic shape) slope distributions averaged over 4 runs performed along the center tangential line within the mirror clear aperture at the pitch angles different by ~140 μrad; (c) the difference between the slope distributions measured at the different pitch angles; and (d) the power spectral density distribution of the difference trace shown in the plot (c).

The plots (a) and (b) in Fig. 9 are results of averaging over two sets of 4 scans performed at the pitch angles differed by ~140 μrad. The systematic error removed by tilting of the mirror is equal to a half of the difference (Fig. 9c) between the traces in Figs. 9a and 9b. The P-V variation of the removed periodic error (the half difference) is about 100 nrad. The power spectral density (PSD) of the difference [plot (d) in Fig. 9] confirms the periodic character of the removed error with the period of ~285 μrad corresponding the periodic systematic error the AC.

7.2.3 Suppression of the drift error by switching the direction of scanning

The efficacy of the applied AOSS to suppression of the error due to the instrumental and set-up drifts can be understood from the repeatability of the measurements.

Figure 10 presents the slope distributions corresponding to the difference of the surface slopes along two sagittally shifted tangential traces measured in two identical runs performed with a delay of about 3 days. The residual slope variation of the difference traces in Fig. 10 is about 22 nrad. The variations have a clear middle spatial frequency character and can be due to the measurement error associated with the periodical variation of the air pressure supplied to the air-bearings of the OSMS gantry system. Note that the amplitude of the PSD peaks of the OSMS repeatability traces in Figs. 10a and 10b is almost two orders of magnitude smaller than that of the removed AC systematic errors (Fig. 9d).

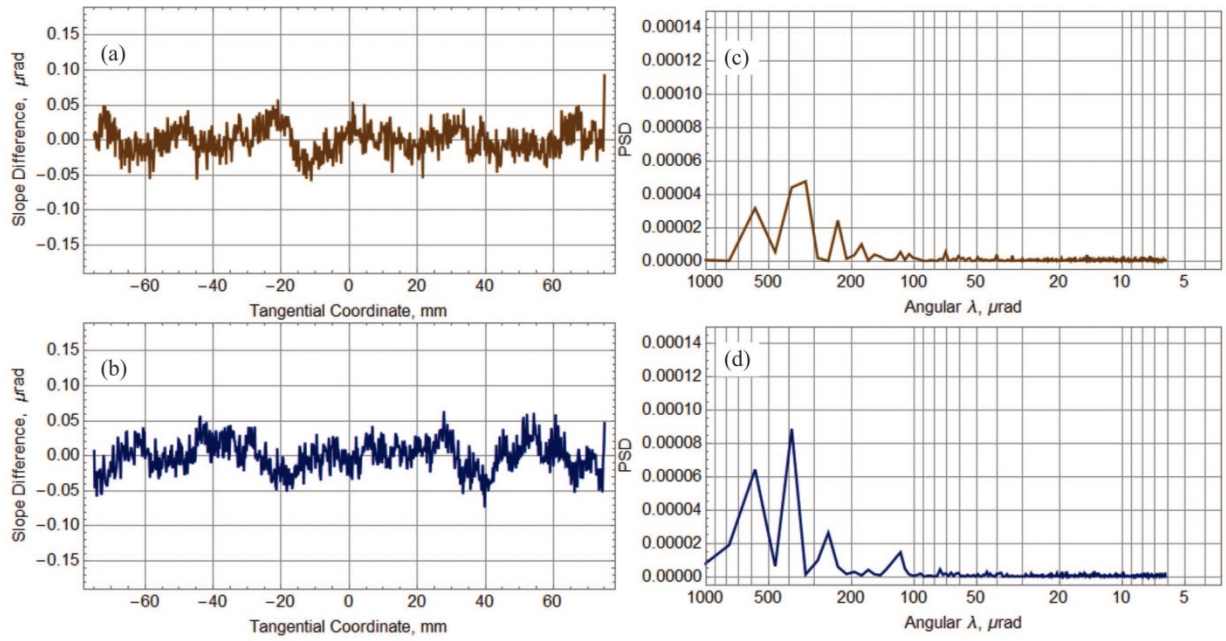

Figure 10: Repeatability of the 2D OSMS surface slope metrology arranged according to the AOSS for a single 8-scan run. (a) and (b): The slope distributions of the difference of the surface slopes along two tangential traces sagittally shifted by ± 5 mm, measured in two identical runs performed with a delay of about 3 days; (c) and (d) the power spectral density distributions corresponding to the difference traces shown in the plots (a) and (b), respectively.

Note that in the measurements discussed here, we did not apply a constant time delay between the scans optimized for suppression of the periodic error related to the air pressure temporal variation, discussed in Sec. 4.3. The corresponding upgrade of the OSMS data acquisition software is in progress.

8. CONCLUSIONS

We have systematically investigated the most efficient, from the point of view of the required funding and achievable advantages, approach for improvement of accuracy of measurements in experimental physics and industry, including ex situ metrology for state-of-the-art x-ray optics. This is the development and implementation of innovative experimental measurement methods for optimal usage of the ultimate capabilities of the existing instrumentation within the available environmental conditions.

We have discussed the key experimental methods and techniques, developed and used at the ALS X-Ray Optical Laboratory, all based on correlation analysis to optimally arrange the acquisition and processing of metrology data. The figure of merit is the maximum suppression of the experimental random noise, instrumental drift, and systematic errors.

We have firstly described an original procedure developed to minimize the measurement errors associated with the periodic temporal variation of the environmental conditions, uncorrelated with the specifics of the measurements, including the position along the SUT and its surface shape. We have shown that by adding a constant delay time between sequential scans of the four-scan OSS run, the periodic error can be significantly suppressed. The analytical expression for proper selection of the optimal delay time has been derived.

We have firstly presented and provided the mathematical foundations for the advanced OSS technique. The AOSS technique allows incorporating, in one measurement run of surface slope metrology, the advantages of the methods for suppression of the random noise, drift and systematic errors, originally applied to a number of sequential runs. Thus in a single eight-scan run arranged according to the AOSS prescription, we get a significant, by a factor of about four, increase of the measurement rate at no degradation of the accuracy of the surface slope metrology.

The high efficacy of the developed advanced optimal scanning strategy technique to suppress measurement errors has been demonstrated in an example of 2D surface slope metrology with a high quality hyperbolic mirror. The metrology was performed at the XROL with a new optical surface measuring system, the ALS OSMS, using an electronic auto-

collimator, ELCOMAT-3000,[82] as a surface slope sensor. It has been shown that in a single 8-scan run arranged according to the corresponding AOSS, we are able to effectively suppress the errors due to the random noise, the instrumental drift, the even part of the systematic errors, and the major periodic systematic error of the OSMS AC.

The resulting tangential slope distributions measured in the OSMS single run are in the excellent agreement with the results of 1D slope measurements with the same hyperbolic cylinder x-ray mirror preliminarily performed using the ALS DLTP[13,14] and OSMS[57] when carrying out the measurements using 4 sequential 8-scan runs, each optimally arranged to solely suppress the drift error. Therefore, the application of the AOSS suggested and described in this paper provides 4-fold improvement of the measurement rate.

Our next goals are to comprehensively test and characterize the performance of the OSMS with the new data acquisition and analysis software (after upgrading the software to the capability to introduce a constant delay between the sequential scans) and to develop a number of different non-contact sensors for the OSMS. The work in these directions is in progress at the ALS XROL.

We should especially emphasize that the developed experimental methods for suppressing the random noise, instrumental drift, and systematic errors in physical measurements are general and applicable to a broad spectrum of high accuracy measurements in experimental science and industry.

ACKNOWLEDGEMENTS

The Advanced Light Source is supported by the Director, Office of Science, Office of Basic Energy Sciences, Material Science Division, of the U.S. Department of Energy under Contract No. DE-AC02-05CH11231 at Lawrence Berkeley National Laboratory.

REFERENCES

[1] ALS-U, https://als.lbl.gov/als-u/ (09 October 2017).
[2] Kevan, S., Chair, [ALS-U: Solving Scientific Challenges with Coherent Soft X-Rays], Workshop report on early science enabled by the Advanced Light Source Upgrade, ALS, LBNL, Berkeley, CA, (2017) https://als.lbl.gov/wp-content/uploads/2017/08/ALS-U-Early-Science-Workshop-Report-Full.pdf (09 October 2017).
[3] Samoylova, L., Sinn, H., Siewert, F., Mimura, H., Yamauchi, K., and Tschentscher, T., "Requirements on Hard X-ray Grazing Incidence Optics for European XFEL: Analysis and Simulation of Wavefront Transformations," Proc. SPIE 7360, 73600E/1-9 (2009).
[4] Assoufid, L., and Rabedeau, T., Co-Chairs, "X-ray Mirrors," in: X-ray Optics for BES Light Source Facilities, Report of the Basic Energy Sciences Workshop on X-ray Optics for BES Light Source Facilities, D. Mills and H. Padmore, Co-Chairs, pp. 118-129, U.S. Department of Energy, Office of Science, Potomac, MD, (2013); http://science.energy.gov/~/media/bes/pdf/reports/files/BES_XRay_Optics_rpt.pdf (09 October 2017).
[5] Yashchuk, V. V., Samoylova, L., and Kozhevnikov, I. V., "Specification of x-ray mirrors in terms of system performance: A new twist to an old plot," Proc. SPIE 9209, 92090F/1-19 (2014).
[6] Yashchuk, V. V., Samoylova, L., and Kozhevnikov, I. V., "Specification of x-ray mirrors in terms of system performance: A new twist to an old plot," Opt. Eng. 54(2), 025108/1-13 (2015).

[7] Cocco, D., “Recent Developments in UV Optics for Ultra-Short, Ultra-Intense Coherent Light Sources,” Photonics 2015, 2(1), 40-49 (2015).
[8] Idir, M. and Yashchuk, V. V., Co-Chairs, “Optical and X-ray metrology,” in [X-ray Optics for BES Light Source Facilities], Report of the Basic Energy Sciences Workshop on X-ray Optics for BES Light Source Facilities, D. Mills and H. Padmore, Co-Chairs, pp. 44-55, U.S. Department of Energy, Office of Science, Potomac, MD (March 27-29, 2013); http://science.energy.gov/~/media/bes/pdf/reports/files/BES_XRay_Optics_rpt.pdf (09 October 2017).
[9] Church, E. L., Takacs, P. Z., "Use of an optical profiling instrument for the measurement of the figure and finish of optical quality surfaces," Wear 109, 241-57 (1986).
[10] Takacs, P. Z., Qian, S., Colbert, J., "Design of a long trace surface profiler," Proc. SPIE 749, 59-64 (1987).
[11] Irick, S. C., “Improved measurement accuracy in a long trace profiler: compensation for laser pointing instability,” Nucl. Instrum. Methods Phys. Res. A 347, 226–230 (1994); https://doi.org/10.1016/0168-9002(94)91882-1.
[12] Takacs, P. Z., Church, E. L., Bresloff, C. J., Assoufid, L., “Improvements in the accuracy and the repeatability of long trace profiler measurements,” Appl. Optics 38(25), 5468-5479 (1999).
[13] Takacs, P. Z., Qian, Shinan, “Accuracy limitations in long-trace profilometry,” AIP Conf. Proc. 708, 831-834 (2004).
[14] Rommeveaux, A., Hignette, O., Morawe, C., “Mirror metrology and bender characterization at ESRF,” Proc. SPIE 5921, 59210N/1-8 (2005).
[15] Kirschman, J. L., Domning, E. E., McKinney, W. R., Morrison, G. Y., Smith, B. V., and Yashchuk, V. V., “Performance of the upgraded LTP-II at the ALS Optical Metrology Laboratory,” Proc. SPIE 7077, 70770A/1-12 (2008).
[16] Rommeveaux, A., Thomasset, M., Cocco, D., “The Long Trace Profilers,” in [Modern Developments in X-ray and Neutron Optics], A. Erko, M. Idir, T. Krist, A. G. Michette, Eds., Chapter 10, Springer-Verlag, Berlin/Heidelberg (2008).
[17] Thomasset M., and Polack, F., “Characterization of optical surfaces for the present generations of synchrotron sources,” Proc. SPIE 7155, 715506/1-12 (2008).
[18] Senba, Y., Kishimoto, H., Ohashi, H., Yumoto, H., Zeschke, T., Siewert, F., Goto, S., Ishikawa, T., “Upgrade of long trace profiler for characterization of high-precision X-ray mirrors at SPring-8,” Nucl. Instrum. and Methods A 616(2-3), 237-240 (2010).
[19] Siewert, F., Noll, T., Schlegel, T., Zeschke, T., and Lammert, H., “The Nanometer Optical Component Measuring machine: a new Sub-nm Topography Measuring Device for X-ray Optics at BESSY,” AIP Conference Proceedings 705, American Institute of Physics, Mellville, NY (2004), pp. 847-850.
[20] Siewert, F., Lammert, H., Zeschke, T., “The Nanometer Optical Component Measuring Machine;” in: [Modern Developments in X-Ray and Neutron Optics], Edited by A. Erko, M. Idir, T. Krist, and A. G. Michette, Springer, New York (2008).
[21] Alcock, S. G., Sawhney, K. J. S., Scott, S., Pedersen, U., Walton, R., Siewert, F., Zeschke, T., Senf, F., Noll T., and Lammert, H., “The Diamond-NOM: A non-contact profiler capable of characterizing optical figure error with sub-nanometre repeatability,” Nucl. Inst. and Methods A 616(2-3), 224-228 (2010).
[22] Yashchuk, V. V., Barber, S., Domning, E. E., Kirschman, J. L., Morrison, G. Y., Smith, B. V., Siewert, F., Zeschke, T., Geckeler, R., Just, A., “Sub-microradian surface slope metrology with the ALS Developmental Long Trace Profiler,” Nucl. Instrum. and Methods A 616(2-3), 212-223 (2010).
[23] Geckeler, R., Just, A., Krause, M. and Yashchuk, V. V., “Autocollimators for Deflectometry: Current Status and Future Progress,” Nucl. Instr. and Meth. A 616(2-3), 140-146 (2010).
[24] Qian, J., Sullivan, J., Erdmann, M., and Assoufid, L., “Performance of the APS optical slope measuring system,” Nucl. Instr. and Meth. A 710, 48-51 (2013); https://doi.org/10.1016/j.nima.2012.10.102.
[25] Nicolas, J., Martínez, J. C., “Characterization of the error budget of Alba-NOM,” Nucl. Instr. and Meth. A 710, 24-30 (2013).
[26] Qian, S., Geckeler, R., Just, A., Idir, M., and Wu, H., “Approaching sub-50 nanoradian measurements by reducing the saw-tooth deviation of the autocollimator in the Nano-Optic-Measuring Machine,” Nucl. Instr. and Meth. A 785, 206-212 (2015); doi: 10.1016/j.nima.2015.02.065.
[27] Yamauchi, K., Yamamura, K., Mimura, H., Sano, Y., Saito, A., Ueno, K., Endo, K., Suovorov, A., Yabashi, M., Tamasaku, K., Ishikawa, T., Mori, Y., "Microstitching interferometry for x-ray reflective optics," Rev. Sci. Instrum. 74, 2894-2898 (2003).

[28] Mimura, H., Yumoto, H., Matsuyama, S., Yamamura, K., Sano, Y., Ueno, K., Endo, K., Mori, Y., Yabashi, M., Tamasaku, K., Nishino, Y., Ishikawa, T., Yamauchi, K., "Relative angle determinable stitching interferometry for hard x-ray reflective optics," Rev. Sci. Instrum. 76, 045102 (2005).
[29] Kimura, T., Ohashi, H., Mimura, H., Yamakawa, D., Yumoto, H., Matsuyama, S., Tsumura, T., Okada, H., Masunaga, T., Senba, Y., Goto, S., Ishikawa, T., Yamauchi, K., "A stitching figure profiler of large X-ray mirrors using RADSI for subaperture data acquisition," Nucl. Instrum. Methods Phys. Res. A 616, 229-232 (2010).
[30] Yamauchi, K., Mimura, H., Kimura, T., Yumoto, H., Handa, S., Matsuyama, S., Arima, K., Sano, Y., Yamamura, K., Inagaki, K., Nakamori, H., Kim, J., Tamasaku, K., Nishino, Y., Yabashi, M., and Ishikawa, T., "Single-nanometer focusing of hard x-rays by Kirkpatrick–Baez mirrors," J. Phys.: Condens. Mattter. 23(39), 394206 (2011); https://doi.org/10.1088/0953-8984/23/39/394206.
[31] MacGovern, A. J. and Wyant, J. C., "Computer Generated Holograms for Testing Optical Elements," Appl. Opt. 10(3), 619-624 (1971).
[32] Birch, K. G. and Green, F. J., "The application of computer-generated holograms to testing optical elements," J. Physics D 5(11), 1982-1994 (1972); http://iopscience.iop.org/0022-3727/5/11/306.
[33] Burge, J. H., "Applications of computer-generated holograms for interferometric measurement of large aspheric optics," Proc. SPIE 2576, 258-269 (1995).
[34] Asfour, J.-M. and Poleshchuk, A. G., "Asphere testing with a Fizeau interferometer based on a combined computer-generated hologram," J. OSA A 23(1), 172-178 (2006); https://doi.org/10.1364/JOSAA.23.000172
[35] A. G. Poleshchuk, V. P. Korolkov, R. K. Nasyrov, J.-M. Asfour, "Computer generated holograms: fabrication and application for precision optical testing", Proc. of SPIE Vol. 7102, 710206/1-9 (2008); doi: 10.1117/12.797816.
[36] Parks, R. E., "Computer Generated Holograms as Fixtures for Testing Optical Elements," in [Design and Fabrication Congress 2017], JTh4B.4.pdf (OSA, 2017); https://doi.org/10.1364/FREEFORM.2017.JTh4B.4.
[37] Alcock, S. G. and Sawhney, K. J. S., "Progress in the X-ray optics and metrology lab at Diamond Light Source," Proc. SPIE 6704, 67040E-1/8 (2007).
[38] Goldberg, K. A., Yashchuk, V. V., Artemiev, N. A., Celestre, R., Chao, W., Gullikson, E. M., Lacey, I., McKinney, W. R., Merthe, D. and Padmore, H. A., "Metrology for the Advancement of X-ray Optics at the ALS," Synchrotron Radiation News 26(5), 4-12 (2013) http://dx.doi.org/10.1080/08940886.2013.832583.
[39] Idir, M., Kaznatcheev, K., Qian, S. and Conley, R., "Current status of the NSLS-II optical metrology laboratory,"Nucl. Instrum. and Methods A 710, 17-23 (2013).
[40] Takacs, P. Z., "X-ray optics metrology," in: [Handbook of Optics], 3rd ed., Vol. V, M. Bass, Ed., Chapter 46, McGraw-Hill, New York (2009).
[41] Yashchuk, V. V., Takacs, P. Z., McKinney, W. R., Assoufid, L., Siewert, F., Zeschke, T., "Development of a new generation of optical slope measuring profiler," Nucl. Instr. and Meth. A 649(1), 153-155 (2011) - LBNL-3975E; http://doi.org/10.1016/j.nima.2010.10.063 Cited: 5 (from Web of Science).
[42] Geckeler, R. D., Kranz, O., Just, A., and Krause, M., "A novel approach for extending autocollimator calibration from plane to spatial angles," Adv. Opt. Techn. 1(6), 427–439 (2012).
[43] Yandayan, T., Ozgur, B., Karaboce, N., and Yaman, O., "High precision small angle generator for realization of the SI unit of plane angle and calibration of high precision autocollimators," Meas. Sci. and Technol. 23(9), 094006/1-12 (2012).
[44] Assoufid, L., Brown, N., Crews, D., Sullivan, J., Erdmann, M., Qian, J., Jemian, P., Yashchuk, V. V., Takacs, P.Z., Artemiev, N. A., Merthe, D. J., McKinney, W. R., Siewert, F., Zeschke, T., "Development of a high-performance gantry system for a new generation of optical slope measuring profilers," Nucl. Instr. and Meth. A 710, 31-36 (2013); http://dx.doi.org/10.1016/j.nima.2012.11.063.
[45] Alcock, S. G., Bugnar, A., Nistea, I., Sawhney, K., Scott, S., Hillman, M., Grindrod, J., and Johnson, I., "A novel instrument for generating angular increments of 1 nanoradian," Rev Sci Instrum. 86(12), 125108 (2015) doi: 10.1063/1.4937352.
[46] Yashchuk, V. V., Artemiev, N. A., Centers, G. P., Chaubard, A., Geckeler, R. D., Lacey, I., Marth, H., McKinney, W. R., Noll, T., Siewert, F., Winter, M., and Zeschke, T., "High precision tilt stage as a key element to universal test mirror for characterization and calibration of slope measuring instruments," Rev. Sci. Instrum. 87(5), 051904 (2016); doi: 10.1063/1.4950729.
[47] Siewert, F., Zeschke, T., Arnold, T., Paetzold, H., and Yashchuk, V. V., "Linear chirped slope profile for spatial calibration in slope measuring deflectometry," Rev. Sci. Instrum. 87(5), 051907/1-8 (2016); doi: 10.1063/1.4950737.

[48] Geckeler, R. D., Artemiev, N. A., Barber, S. K., Just, A., Lacey, I., Kranz, O., Smith, B. V., and Yashchuk, V. V., "Aperture alignment in autocollimator-based deflectometric profilometers," Rev. Sci. Instrum. 87(5), 051906/1-8 (2016); doi: 10.1063/1.4950734.
[49] Yashchuk, V. V., Artemiev, N. A., Lacey, I., McKinney, W. R. and Padmore, H. A., "Advanced environmental control as a key component in the development of ultra-high accuracy ex situ metrology for x-ray optics," Opt. Eng. 54(10), 104104/1-14 (2015); doi: 10.1117/1.OE.54.10.104104.
[50] Yashchuk, V. V., Artemiev, N. A., Lacey, I., McKinney, W. R. and Padmore, H. A., "A new X-ray optics laboratory (XROL) at the ALS: Mission, arrangement, metrology capabilities, performance, and future plans," Proc. SPIE 9206, 92060I/1-19 (2014); doi:10.1117/12.2062042.
[51] McKinney, W. R. and Irick, S. C. "XUV synchrotron optical components for the Advanced Light Source: Summary of the requirements and the developmental program," Proc. SPIE. 1740, 154-160 (1993); doi: 10.1117/12.138697.
[52] Irick, S. C. "Error Reduction Techniques for Measuring Long Synchrotron Mirrors," Proc. SPIE 3447, 101-108 (1998); doi: 10.1117/12.331122.
[53] Yashchuk, V. V., "Optimal measurement strategies for effective suppression of drift errors," Rev. Sci. Instrum. 80, 115101-10 (2009); doi: 10.1063/1.3249559.
[54] Polack, F., Thomasset, M., Brochet, S., and Rommeveaux, A., "An LTP stitching procedure with compensation of instrument errors: Comparison of SOLEIL and ESRF results on strongly curved mirrors," Nucl. Instr. and Met. A 616(2-3), 207-211 (2010); doi:10.1016/j.nima.2009.10.166.
[55] Yashchuk, V. V., Artemiev, N. A., Lacey, I., and Merthe, D. J., "Correlation analysis of surface slope metrology measurements of high quality x-ray optics," Proc. SPIE 8848, 884817-1-15 (2013).
[56] Nicolas, J., Pedriera, P., Sics, I., Ramirez, C., and Campos, J., "Nanometer accuracy with continuous scans at the ALBA-NOM," Proc. SPIE 9962, Advances in Metrology for X-Ray and EUV Optics VI, 996203 (2016); doi:10.1117/12.2238128.
[57] Lacey, I., Adam, J., Centers, G., Gevorkyan, G. S., Nikitin, S. M., Smith, B. V., and Yashchuk, V. V., "Development of a high performance surface slope measuring system for two-dimensional mapping of x-ray optics,"Proc. SPIE 10385, 10385 – 16/1-13(2017).
[58] Yashchuk, V. V., Irick S. C., MacDowell, A. A., McKinney, W. R., and Takacs, P. Z., "Air convection noise of pencil-beam interferometer for long-trace profiler," Proc. SPIE 6317, 63170D-1-12 (2006); doi: 10.1117/12.681297.
[59] Lacey, I., Artemiev, N. A., Domning, E. E., McKinney, W. R., Morrison, G. Y., Morton, S. A., Smith, B. V., and Yashchuk, V. V., "The developmental long trace profiler (DLTP) optimized for metrology of side-facing optics at the ALS," Proc. SPIE 9206, 920603/1-11 (2014); doi:10.1117/12.2061969.
[60] Siewert, F., Buchheim, J., and Zeschke, T., "Characterization and calibration of 2nd generation slope measuring profiler," Nucl. Instrum. Methods A 616(2-3), 119–127 (2010); http://doi.org/10.1016/j.nima.2009.12.033.
[61] Yashchuk, V. V., McKinney, W. R., Warwick, T., Noll, T., Siewert, F., Zeschke, T., and Geckeler, R. D., "Proposal for a Universal Test Mirror for Characterization of Slope Measuring Instruments," Proc. SPIE 6704, 67040A-1-12 (2007).
[62] Yashchuk, V. V., Artemiev, N. A., Centers, G., Chaubard, A., Geckeler, R. D., Lacey, I., Marth, H., McKinney, W. R., Noll, T., Siewert, F., Winter, M., and Zeschke, T., "High precision tilt stage as a key element to universal test mirror for characterization and calibration of slope measuring instruments," Rev. Sci. Instrum. 87(5), 051904 (2016); doi: 10.1063/1.4950729.
[63] Qian, S., Sostero, G., Takacs, P. Z., "Precision calibration and systematic error reduction in the long trace profiler," Opt. Eng. 39(1), 304-310 (2000); doi: 10.1117/1.602364.
[64] Nikitin, S. M., Gevorkyan, G. S., McKinney, W. R., Lacey, I., Takacs, P. Z., and V. V. Yashchuk, "New twist in the optical schematic of surface slope measuring long trace profiler," Proc. SPIE 10385, 10385 – 19/1-17 (2017).
[65] Yashchuk, V. V., "Positioning errors of pencil-beam interferometers for long trace profilers," Proc. SPIE 6317, 63170A/1-12 (2006).
[66] Ali, Z., Artemiev, N. A., Cummings, C. L., Domning, E. E., Kelez, N., McKinney, W. R., Merthe, D. J., Morrison, G. Y., Smith, B. V., and Yashchuk, V. V., "Automated suppression of errors in LTP-II slope measurements with x-ray optics," Proc. SPIE 8141, 81410O-1-15 (2011).
[67] Harrison, G. E., Player, M. A., and Sandars, P. G. H., "A multichannel phase-sensitive detection method using orthogonal square waveforms," J. Phys. E 4, 750 (1971).
[68] Harrison, G. E., Sandars, P. G. H., and Wright, S. J., "Experimental limit on the proton electric dipole moment," Phys. Rev. Lett. 22, 1263 (1969).

[69] Player, M. A., and Sandars, P. G. H., "An experiment to search for an electric dipole moment in the $^3P_2$ metastable state of xenon," J. Phys. B 3, 1620 (1970).
[70] Altarev, S., Borisov, Yu. V., Borovikova, N. V., Egorov, A. I., Ivanov, S. N., Kolomensky, E. A., Lasakov, M. S., Lobashev, V. M., Nazarenko, V. A., Pirozhkov, A. N., Serebrov, A. P., Sobolev, Yu. V., and Shulgina, E. V., "Search for the neutron electric dipole moment," Phys. At. Nucl. 59, 1152- 1170 (1996); http://dx.doi.org/10.1134/1.854647.
[71] Baker, C. A., Doyle, D. D., Geltenbort, P., Green, K., van der Grinten, M. G. D., Harris, P. G., Iaydjiev, P., Ivanov, S. N., May, D. J. R., Pendlebury, J. M., Richardson, J. D., Shiers, D., and Smith, K. F., "Improved Experimental Limit on the Electric Dipole Moment of the Neutron," Phys. Rev. Lett. 97, 131801 (2006); doi: 10.1103/PhysRevLett.97.131801.
[72] Serebrov, A. P., Kolomenskiy, E. A., Pirozhkov, A. N., Krasnoshekova I. A., Vasiliev, A. V., Polyushkin, A. O., Lasakov, M. S., Murashkin, A. N., Solovey, V. A., Fomin, A. K., Shoka, I. V., Zherebtsov, O. M., Geltenbort, P., Ivanov, S. N., Zimmer, O., Alexandrov, E. B., Dmitriev, S. P., and Dovator, N. A., "New measurements of the neutron electric dipole moment with the Petersburg Nuclear Physics Institute double-chamber electric dipole moment spectrometer," Phys. of Particles and Nuclei Lett. 12(2), 286–296 (2015); doi: 10.1134/S1547477115020193.
[73] Regan, B. C., Commins, E. D., Schmidt, C. J., and DeMille, D., "New limit on the electron electric dipole moment," Phys. Rev. Lett. 88, 071805 (2002); doi: 10.1103/PhysRevLett.88.071805.
[74] Griffith, W. C., Swallows, M. D., Loftus, T. H., Romalis, M. V., Heckel, B. R., and Fortson, E. N., "Improved Limit on the Permanent Electric Dipole Moment of ^{199}Hg," Phys. Rev. Lett. 102, 101601 (2009); https://doi.org/10.1103/PhysRevLett.102.101601.
[75] Murthy, S. A., Krause, D., Li, Z. L., and Hunter, L. R., "New limits on the electron electric dipole moment from cesium," Phys. Rev. Lett. 63, 965 (1989); https://doi.org/10.1103/PhysRevLett.63.965.
[76] Hinds, E. A. and Sandars, P. G., "Experiment to search for P- and T-violating interactions in the hyperfine structure of thallium fluoride," Phys. Rev. A 21, 480-487 (1980); https://doi.org/10.1103/PhysRevA.21.480.
[77] Hudson, J. J., Sauer, B. E., Tarbutt, M. R., and Hinds, E. A., "Measurement of the electron electric dipole moment using YbF molecules," Phys. Rev. Lett. 89, 023003 (2002); https://doi.org/10.1103/PhysRevLett.89.023003.
[78] Baron, J., Campbell, W. C., DeMille, D., Doyle, J. M., Gabrielse, G., Gurevich, Y. V., Hess, P. W., Hutzler, N. R., Kirilov, E., Kozyryev, I., O'Leary, B. R., Panda, C. D., Parsons, M. F., Petrik, E. S., Spaun, B., Vutha, A. C., and West, A. D., "Order of magnitude smaller limit on the electric dipole moment of the electron," Science 343, 269-272 (2014); doi: 10.1126/science.1248213.
[79] Heidenreich, B. J., Elliott, O. T., Charney, N. D., Virgien, K. A., Bridges, A. W., McKeon, M. A., Peck, S. K., Krause, D., Gordon, J. E., Hunter, L. R., and Lamoreaux, S. K., "Limit on the electron electric dipole moment in gadolinium-iron garnet," Phys. Rev. Lett. 95, 253004 (2005); https://doi.org/10.1103/PhysRevLett.95.253004.
[80] Q-Sys, [The company], http://www.q-sys.eu/the_company.html (09 October 2017).
[81] Warwick, T., Anderson, C., Gaines, G., Yashchuk, V., Voronov, D., Chuang, Yi-De, and Padmore, H., "Optical and Mechanical Tolerances for QERLIN Spectrometer," LSBL Note LSBL-1279RevA (Berkeley, October, 2015).
[82] MÖLLER-WEDEL OPTICAL GmbH, [ELCOMAT-3000], https://www.haag-streit.com/moeller-wedel-optical/products/electronic-autocollimators/elcomat-series/elcomat-3000/#c3723 (09 October 2017).